Environment and Ecology 44 (1) 132—150, January—March 2026
Article DOI: https://doi.org/10.60151/envec/JZNN3612
ISSN: 0970-0420 (Print), ISSN: 3049-3625 (Online)

Blue Carbon Dynamics and Vegetation Structure of Urban-Edge Mangroves along the Ulhas River–Vasai–Thane Creek Estuary, India

Madhuri R. Wani, D. M. Mahajan, Deepavali Shirurkar

Received 7 January 2026, Accepted 26 February 2026, Published on 19 March 2026

ABSTRACT

Urban-edge mangroves represent critical yet increasingly vulnerable blue-carbon ecosystems, particularly within rapidly urbanizing estuarine landscapes. However, integrated assessments linking vegetation structure, biomass carbon, soil organic carbon (SOC), and ecosystem service value at the municipal scale remain limited in India. Vegetation structure and species dominance were assessed using phytosociological indices within fixed-area quadrats along the Ulhas River–Vasai–Thane Creek estuarine system in the Kalyan–Dombivli Municipal Corporation (KDMC) region. Species-wise biomass and carbon stocks were estimated using growth-form–appropriate allometric equations, while SOC stocks were quantified for two depth intervals (0–15 cm and 15–30 cm) using standard laboratory procedures. Relationships between species ecological importance and biomass carbon contribution were examined using descriptive graphical analysis. The mangrove assemblage was dominated by disturbance-tolerant shrubs and climbers, particularly *Acanthus ilicifolius* and *Derris trifoliata,* while canopy-forming trees (*Avicennia officinalis* and *Sonneratia apetala*) were less abundant but structurally significant. Biomass carbon storage was disproportionately governed by these canopy-forming species, whereas shrub and liana dominated components exhibited high ecological dominance but comparatively low carbon contribution. SOC constituted the dominant and more stable carbon pool, with significantly higher stocks in subsurface layers (15–30 cm) than in surface soils, highlighting effective long-term carbon burial. Marked spatial variability in SOC stocks reflected differences in hydrological connectivity and disturbance intensity across sites. Urban-edge mangroves within KDMC function as ecologically resilient yet carbon-fragile systems, where sedimentary carbon pools play a critical role in long-term carbon storage. Species dominance alone is an insufficient proxy for biomass carbon sequestration without consideration of growth form and structural attributes. Protection of canopy-forming mangrove trees, maintenance of tidal connectivity, and prevention of sediment disturbance are essential to sustain blue-carbon functions in urban estuarine environments. This study provides a robust baseline for integrating urban mangroves into municipal climate mitigation and coastal resilience planning.

Keywords Biomass carbon, Blue carbon, Coastal resilience, Estuarine ecosystems, Phytosociology, Soil organic carbon, Urban mangroves.

Madhuri R. Wani[1], D. M. Mahajan[2]*, Deepavali Shirurkar[3]

[1]PhD Research Scholar, [2]Professor, [3]Retired Professor
[1,3]Environmental Science Research Centre, Baburaoji Gholap College, Sangvi, Pune 411027, (Affiliated to Savitribai Phule Pune University, India)

[2]Department of Botany, Anantrao Pawar College, Pirangut, Dist. Pune, (Affiliated to Savitribai Phule Pune University, India)

Email: mahajandm@gmail.com
*Corresponding author

INTRODUCTION

Mangrove ecosystems represent one of the most carbon-dense coastal forest types globally and play a disproportionate role in climate regulation, shoreline stabilization, sediment trapping, nutrient cycling, and fisheries productivity (Donato *et al.* 2011, Alongi 2014, Ouyang *et al.* 2017, Atwood *et al.* 2017, IPCC 2019, Alongi 2020, Kauffman *et al.* 2020). Their capacity to sequester and store carbon in both biomass and sediments, commonly termed 'blue carbon', far exceeds that of most terrestrial tropical forests on a per-unit-area basis (Komiyama *et al.* 2008, Brander *et al.* 2012, Atwood *et al.* 2017, Macreadie *et al*. 2021, IPCC 2019, Kauffman *et al.* 2020). However, mangroves are undergoing rapid degradation worldwide due to coastal urbanization, land reclamation, aquaculture expansion, pollution, and hydrological modification (Salem and Mercer 2012, Mukherjee *et al.* 2014, Taillardat *et al.* 2018, Getzner and Islam 2020, FSI 2021, Bandh *et al.* 2023). These pressures diminish floral diversity and stand structure and destabilize long-term carbon stores, posing a dual threat to biodiversity conservation and climate-change mitigation (Harris *et al.* 2010, Friess *et al.* 2016a, NCSCM 2017, Lee *et al.* 2014, Kannankai *et al.* 2022, Szafranski and Granek 2023).

In India, mangrove forests occupy approximately 4,975 km² and are distributed along both the east and west coasts. Western Indian mangroves form narrow, fragmented belts embedded within estuarine and deltaic systems (Kumar 2025). Over the last two decades, intensified coastal development, port expansion, urban sprawl, and infrastructure growth have exerted unprecedented pressure on west-coast mangroves, particularly within the Mumbai Metropolitan Region (MMR) (Curtis and McIntosh 1950, Rani *et al*. 2023, Singh *et al.* 2023). Recent studies from Kachchh (Gujarat), Pichavaram (Tamil Nadu), and the Indian Sundarbans demonstrate that rapid land-use change and anthropogenic stress can significantly alter mangrove vegetation structure, carbon stocks, and ecosystem service delivery, even when forest cover appears visually intact (Ghosh *et al*. 2022, Dutta *et al.* 2022, IPCC 2006, Thivakaran *et al.* 2020, Chaudhuri *et al.* 2023). Despite these advances, urban-edge mangrove fragments embedded within rapidly expanding municipal landscapes remain underrepresented in India's blue-carbon literature, particularly in the context of municipal-scale planning.

The Kalyan–Dombivli Municipal Corporation (KDMC) region along the Ulhas River–Vasai–Thane Creek estuarine system is one of the fastest urbanizing coastal belts of the MMR. Mangroves within KDMC occur as narrow, discontinuous patches subjected to embankment construction, solid-waste dumping, informal settlements, hydrological obstruction, and shoreline hardening (Alongi 2015, 2022). Unlike relatively intact mangrove landscapes, these urban-edge mangroves persist under chronic anthropogenic stress yet continue to deliver critical ecological functions such as sediment stabilization, flood buffering, nutrient processing, and carbon sequestration. However, quantitative site-specific information on phytosociology, biomass carbon, soil organic carbon (SOC), and integrated ecosystem service valuation (ESV) for KDMC mangroves has been virtually absent.

Blue-carbon research in India has expanded in recent years, but most studies have focused on either floristics, remote-sensing-based area change, or isolated carbon pool estimation (Satyanarayana *et al*. 2002, Shindikar *et al*. 2009, Pachpande and Pejaver 2015, Vinod *et al.* 2018, Kamruzzaman *et al.* 2018, Harishma *et al.* 2020, Panditrao 2020, Arathy *et al.* 2022). Few investigations have integrated vegetation structure, biomass carbon, SOC stratification, and economic valuation within the same spatial framework, especially for urban-edge mangrove systems where degradation trajectories differ fundamentally from those of protected reserves. Recent work emphasizes the need for such integrated baselines to support nature-based climate solutions, urban resilience planning, and India's Nationally Determined Contributions (NDCs) (Nagelkerken *et al.* 2008, Friess *et al.* 2016b, Singh *et al.* 2023, Sumarga *et al.* 2023).

Accordingly, the present study addresses four critical research gaps in the KDMC mangroves: i) lack of detailed phytosociological characterization of urban-edge mangroves under chronic disturbance, ii) limited biomass and species-level carbon estimates for structurally dominant shrubs, lianas, and trees in urban mangrove systems, iii) insufficient station-wise

SOC stock data for both shallow and subsurface soil layers in municipal mangrove landscapes, and iv) absence of benefit-transfer–based ecosystem service valuation explicitly linked to blue-carbon stocks in KDMC.

The specific objectives of this study were to: i) quantify species composition, diversity, and structural attributes of urban-edge mangroves using standard phytosociological indices, ii) estimate aboveground biomass (AGB), belowground biomass (BGB), and associated carbon fractions using allometric relationships, iii) determine SOC concentrations and SOC stocks at 0–15 cm and 15–30 cm depths across representative stations, and iv) derive a first-order benefit-transfer-based valuation of ecosystem services (with uncertainty bounds) associated with the mangrove blue-carbon stock.

By integrating vegetation structure, biomass carbon, SOC, and ecosystem service valuation within a unified framework, this study provides the first integrated, policy-relevant blue-carbon baseline for the urban-edge mangroves of the Kalyan–Dombivli region. The findings offer critical scientific inputs for municipal climate-action planning, coastal zone management, and the fulfillment of India's NDCs.

MATERIALS AND METHODS

Study area

The investigation was conducted along urban-edge mangrove stretches fringing the Ulhas River–Vasai–Thane Creek estuarine system, within the administrative limits of KDMC, Maharashtra, India. The mangrove extent of this area was mapped to be approximately 200 ± 20 ha (Fig. 1). The KDMC region forms a rapidly urbanizing segment of the Mumbai Metropolitan Region and is characterized by intense land-use transformation driven by residential expansion, industrial development, transportation infrastructure, and shoreline modification. The climate is humid tropical monsoonal, with annual rainfall ~2,500 mm concentrated between June and September and a mean annual temperature of ~27.5 °C. Tidal regimes are semidiurnal and strongly influence salinity gradients, sediment deposition, and nutrient exchange across the mangrove belt. Geomorphology is dominated by low-lying intertidal mudflats, tidal creeks, and reclaimed lands. Mangroves occur as narrow, highly fragmented belts bordering the

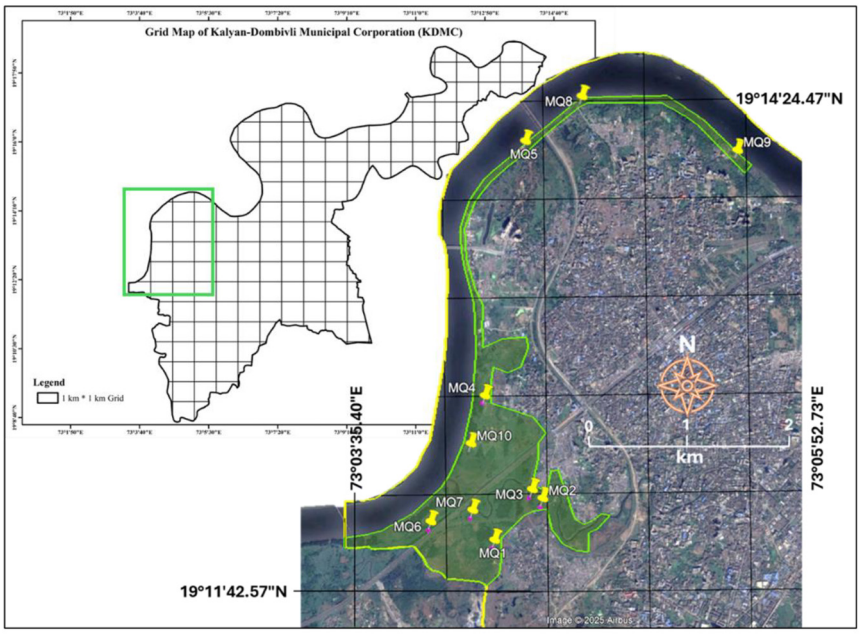

Fig. 1. Spatial extent and distribution of mangrove vegetation along the Ulhas River estuarine system.

estuarine channels and are subjected to continuous anthropogenic pressures, including embankment construction, solid-waste dumping, sewage inflow, shoreline encroachment, and restricted tidal flushing.

Phytosociological assessment

Sampling design and quadrat layout

Vegetation sampling was conducted using a stratified quadrat-based approach to capture the full range of disturbance intensities and tidal zonation across the KDMC mangrove belt. Stratification criteria included: (i) proximity to urban infrastructure and waste-disposal zones, (ii) frequency of tidal inundation, and (iii) apparent canopy condition. Ten representative urban-edge mangrove sampling stations were selected to encompass a gradient of hydrological connectivity, pollution intensity, sediment texture, and urban disturbance.

Within each station, a 15 m×15 m quadrat (225 m²) was established using constrained random placement, accounting for accessibility and safety on soft mud substrates, waterlogging, and waste accumulation. The relatively large quadrat size was chosen to capture the vertical and horizontal structural variability of these degraded mangroves, which include scattered tree individuals, dense understory shrub thickets (primarily *Acanthus ilicifolius*), and extensive liana networks (*Derris trifoliata*) that smaller quadrats might underestimate. In total, 10 quadrats (n = 10) were sampled. Within each quadrat, all woody individuals with girth at breast height (GBH) ≥ 10 cm were enumerated and identified to species level using standard regional floras.

Measurement of dendrometric variables

For tree species, GBH was measured at 1.3 m above ground using a diameter tape, avoiding buttress swellings and major branch junctions. For shrubby species like *Acanthus ilicifolius* and liana species like *Derris trifoliata,* basal stem diameter was measured at 30–50 cm above ground (depending on the point of first stem consolidation). In entangled liana mats, individual ramets were distinguished based on discrete rooting points, and each measurable climbing stem was recorded separately to avoid overestimation. Tree height was measured for all structurally dominant species using a clinometer and graduated pole method (Martin 2022) along a clear line of sight. For shrubs and lianas, total stem length was measured using flexible measuring tapes along the primary climbing axis.

Computation of phytosociological parameters

Standard phytosociological parameters were computed for each species (Curtis and McIntosh 1950, Mueller-Dombois and Ellenberg 1974): Frequency (F), Density (D), Basal Area (BA), Relative Frequency (RF), Relative Density (RD), and Relative Dominance (RDo). Basal area was calculated from stem circumference (assuming circular cross-sections). Relative dominance was derived from each species' BA contribution and was not conflated with density. The Importance Value Index (IVI) for each species was calculated as the sum of RF, RD, and RDo. Species were classified as true mangroves or mangrove associates based on established floristic criteria. Vegetation diversity was evaluated using the Shannon–Wiener diversity index (H′) and Simpson's dominance index (D),

where:

Shannon–Wiener diversity index (H′):

$$H' = -\sum(p_i \ln p_i)$$

Simpson's dominance index (D):

$$D \sum \left(\frac{n_i (n_i - 1)}{N (N - 1)} \right)$$

where p_i is the proportional abundance of species i., n_i is the number of individuals in the i^{th} species, and N = the total number of individuals. As D increases, diversity decreases and Simpson index is therefore usually expressed as 1-D or 1/D. These indices were interpreted as integrative measures of richness–evenness structure and dominance, not as direct measures of species richness alone.

Biomass and carbon estimation

Selection of species and dendrometric dataset

Biomass estimation was performed for all structurally

dominant woody shrub, and liana species contributing significantly to total stand IVI. These included *Avicennia officinalis, Sonneratia apetala, Derris trifoliata, Acanthus ilicifolius, Excoecaria agallocha, Bruguiera cylindrica, Pithecellobium dulce, Bombax ceiba, Morinda citrifolia,* and *Leucaena leucocephala.* In total, 177 individuals (n = 177) were measured and included in the biomass estimation dataset.

Allometric equations and parameterization

Aboveground biomass (AGB) was estimated using species-specific mangrove allometric equations where available (Komiyama *et al.* 2008, Chave *et al.* 2014, Kusmana *et al.* 2018). Species-appropriate models were prioritized to ensure accurate representation of mangrove architecture and biomass allocation patterns. For non-arborescent growth forms, specifically shrubs (*Acanthus ilicifolius*) and lianas (*Derris trifoliata*), shrub- and climber-specific allometric equations (Schnitzer *et al.* 2006) were applied cautiously, to minimize the overestimation bias known to occur when tree-based models are applied to non-tree vegetation (Chave *et al*. 2014).

Komiyama *et al.*'s (2008) allometric equations for mangrove species in Southeast Asia were employed for AGB and belowground biomass (BGB) as follows:

$$AGB = 0.251\ \rho\ D^{2.46}$$
$$BGB = 0.199\ \rho^{0.899}\ D^{2.22}$$

where ρ is species-specific wood density (g cm^{-3}) and D is stem diameter (cm). Wood density values for each mangrove species were obtained from global databases (Chave *et al.* 2009). Estimated AGB and BGB per individual were summed to derive total biomass per quadrat, which was then scaled to tonnes per hectare (t ha^{-1}).

Biomass carbon content was calculated by multiplying individual biomass by a carbon conversion factor of 0.5, following IPCC (2006) guidelines. Understory vegetation (seedlings and herbaceous components) was excluded from ecosystem-level carbon stock estimation due to its negligible contribution in mangroves (Kauffman and Donato 2012, Vinod *et al.* 2018). For any non-mangrove tree species encountered (e.g., *Pithecellobium dulce, Leucaena*), a generalized allometric equation was used:

$$AGB = a \times (\rho \times D^2 \times H)^b$$

where ρ is wood density (g cm^{-3}), D is stem diameter (cm), H is total height (m), and a and b are empirically derived model coefficients. BGB for these was estimated using species-appropriate root-to-shoot ratios. Species-level wood density values were used when available, otherwise, genus-level mean values were substituted, with such cases noted as potential sources of uncertainty.

All field and derived measurements were cross-checked for unit consistency (e.g., cm to m conversions, cm^2 to m^2 for area) to prevent scaling errors. Biomass carbon stock per quadrat was also expressed in carbon dioxide equivalent (CO_2e) by multiplying C mass by 44/12 (the ratio of molecular weight of CO_2 to carbon). All biomass, carbon stock, and CO_2e estimates are reported with two-decimal precision for consistency and comparability.

Soil Organic Carbon (SOC) sampling and analysis

Sampling scheme

Soil organic carbon was assessed at the 10 mangrove stations following standard protocols (FAO 2006, IPCC 2019). At each station, soil samples were collected from two ecologically relevant depth intervals: 0–15 cm and 15–30 cm, reflecting the surface organic-rich layer and the immediate subsurface. Multiple subsamples per depth at each site were composited to account for within-quadrat heterogeneity. Samples were taken in waterlogged conditions typical of mangrove sediments, and care was taken to avoid compaction during sampling.

Laboratory analysis

Samples were air-dried and sieved (2 mm) before SOC analysis using the Walkley–Black wet oxidation method (Walkley and Black 1934), which involves oxidation of organic carbon with potassium dichromate and sulfuric acid, followed by titration.

A correction factor of 1.33 was applied to adjust for incomplete organic carbon oxidation inherent in the Walkley–Black method. SOC concentration (as % of dry soil) was converted to SOC stock (t C ha^{-1}) by multiplying by bulk density (BD) and the depth interval (15 cm). Bulk density was determined from the dry mass of a known-volume soil core. SOC stock was computed using the standard equation:

$$SOC_{stock} = SOC\ (\%) \times BD \times Depth\ (cm) \times 0.1$$

Statistical analysis

Statistical analyses were conducted using Microsoft Excel and R (R Core Team 2023). Descriptive statistics (mean, median, standard deviation, interquartile range) were computed for all major variables. Data normality was tested with the Shapiro–Wilk test. Relationships between variables were evaluated using Pearson's correlation for normally distributed data and Spearman's rank correlation for non-parametric assessment. Inter-station differences were tested with one-way ANOVA (for parametric data) or Kruskal–Wallis tests (for non-parametric). Statistical significance was evaluated at $\alpha = 0.05$ unless stated otherwise. Correlation coefficients (r), test statistics (e.g., t or F), degrees of freedom, and p-values are reported where relevant.

Spatial analysis and uncertainty characterization

Mangrove areal extent was mapped via on-screen digitization of recent high-resolution Google Earth imagery in a GIS environment. Given the challenges of delineating patchy mangrove fragments, an uncertainty range of ±10–20 ha (~±10%) was applied to the area estimate to account for geolocation error and interpreter bias. All point locations (e.g., sampling stations) were recorded with a handheld GPS (WGS 84 datum).

Ecosystem Service Valuation (ESV)

Mangrove ecosystem service value was estimated using a benefit-transfer approach (Brander *et al.* 2012, Salem and Mercer 2012, Getzner and Islam 2020). A global average ecosystem service value per unit area for mangroves (in US$ ha^{-1} yr^{-1}) was applied to the KDMC mangrove area (~200 ha) to estimate total annual ESV. Three scenarios were considered: a conservative lower bound (using the lower 25th percentile of global mangrove values), a global mean scenario, and an upper bound (using the 75th percentile). A sensitivity analysis was conducted by varying the unit value by ±25% and the area by ±10% to gauge the robustness of the ESV estimate against uncertainties in both the economic coefficients and mapped area. All monetary values are reported in US$ per year, and results are rounded to three significant figures.

RESULTS

Species composition, structural attributes, and dominance pattern

A total of ten woody and shrubby species (eight families) were recorded in the KDMC urban-edge mangrove belt (Table 1). The flora comprises both true mangrove species (*Avicennia officinalis, Sonneratia apetala, Bruguiera cylindrica, Excoecaria agallocha*) and mangrove associates (*Acanthus ilicifolius, Derris trifoliata, Pithecellobium dulce, Bombax ceiba, Morinda citrifolia, Leucaena leucocephala*), indicating a structurally mixed, disturbance-influenced assemblage.

The Relative Frequency values indicate a broad distribution for *Avicennia officinalis, Sonneratia apetala*, and *Derris trifoliata* (each 21.43%), reflecting their presence across most quadrats. In contrast,

Table 1. Phytosociological attributes of mangrove vegetation along the Ulhas River (KDMC).

Species	Relative Frequency (%)	Relative Density (%)	Relative Dominance (%)	IVI
Acanthus ilicifolius	14.29	49.15	33.460	96.90
Avicennia officinalis	21.43	10.17	32.716	64.31
Derris scandens	21.43	24.86	17.416	63.70
Sonneratia apetala	21.43	7.91	16.285	45.62
Pithecellobium dulce	4.76	1.13	0.023	5.92
Bombax ceiba	4.76	1.13	0.010	5.90
Morinda citrifolia	4.76	1.13	0.006	5.90
Excoecaria agallocha	2.38	2.26	0.047	4.69
Bruguiera cylindrica	2.38	1.69	0.035	4.11
Leucaena leucocephala	2.38	0.56	0.001	2.95

Excoecaria agallocha, Bruguiera cylindrica, and *Leucaena leucocephala* had very low frequency (2.38% each), indicating highly localized occurrences. Relative Density showed a clear numerical dominance of *Acanthus ilicifolius* (49.15%), followed by *Derris trifoliata* (24.86%) and *Avicennia officinalis* (10.17%), together these three accounted for over 84% of all stems. Each remaining species contributed under 3% of total stem count.

Patterns of Relative Dominance (based on basal area) revealed that *Acanthus ilicifolius* (33.46%) and *Avicennia officinalis* (32.72%) were the principal contributors to stand basal area, followed by *Derris trifoliata* (17.42%) and *Sonneratia apetala* (16.29%). All other species had minimal basal area contributions (<0.05% each). The combined effect of frequency, density, and dominance is reflected in the Importance Value Index (IVI): *Acanthus ilicifolius* attained the highest IVI (96.90), confirming its overwhelming structural and numerical dominance in this urban-edge mangrove system. *Avicennia officinalis* (64.31) and *Derris trifoliata* (63.70) formed a co-dominant assemblage, while *Sonneratia apetala* (45.62) functioned as a sub-dominant canopy species. All other taxa had IVI < 6, signifying ecologically minor roles. The Shannon–Wiener diversity index (H′ = 1.23) and Simpson's dominance index (D = 0.63, or 1 – D = 0.37) depict a community of moderate species diversity but strong dominance by a few species, a pattern typical of disturbed urban-edge mangroves where evenness is reduced and certain tolerant species predominate.

Species-wise biomass distribution and biomass–carbon sequestration

Biomass and carbon stocks for the inventoried 177 individuals are summarized in Table 2. The total measured aboveground biomass (AGB) was 1,811.8 t, and total belowground biomass (BGB) was 498.84 t, yielding a combined stand biomass of ~2,310.65 t (across ~200 ha). This corresponds to an estimated biomass carbon stock of ~1,086.01 t C (≈3,981.29 t CO_2 equivalent).

Among the true mangroves, *Avicennia officinalis* was the largest contributor to total biomass and carbon stock, with ~956.61 t AGB, 267.85 t BGB, and ~575.50 t C (approximately 52% of the total biomass carbon pool). *Sonneratia apetala* ranked second with ~431.94 t AGB, 120.94 t BGB, and ~259.86 t C (~24% of total biomass C). The climber Derris trifoliata (though a non-tree life form) contributed ~205.85 t C (~19%), reflecting its high stem density, while the shrub *Acanthus ilicifolius* contributed ~43.94 t C (~4%). All remaining associate species together accounted for <1% of total biomass carbon, underscoring the disproportionate contribution of a few dominant taxa to overall carbon sequestration. The stand-level AGB:BGB ratio was ~3.85, indicating about 20.6% of total biomass is allocated belowground, substantial root biomass allocation even under degraded, urban-edge conditions.

Relationship between species importance (IVI) and biomass-carbon contribution

The relationship between species ecological impor-

Table 2. Species-wise biomass and carbon stocks in KDMC mangrove.

Botanical Name	Individuals	Wood Density (kg/m³)	AGB (t)	BGB (t)	Total Biomass (t)	Carbon Fraction (t C)	CO_2 Equivalent (t)
Avicennia officinalis	18	600.0	956.61	267.85	1,224.46	612.23	2,109.77
Sonneratia apetala	14	550.0	431.94	120.94	552.89	276.45	952.63
Derris trifoliata	44	450.0	347.60	90.38	437.98	218.99	754.65
Acanthus ilicifolius	87	450.0	74.20	19.29	93.49	46.75	161.09
Pithecellobium dulce	2	650.0	0.57	0.15	0.72	0.36	1.23
Excoecaria agallocha	4	550.0	0.38	0.10	0.48	0.24	0.83
Bruguiera cylindrica	3	690.0	0.35	0.09	0.44	0.22	0.76
Bombax ceiba	2	330.0	0.09	0.02	0.11	0.06	0.19
Morinda citrifolia	2	450.0	0.04	0.01	0.05	0.03	0.09
Leucaena leucocephala	1	560.0	0.02	0.01	0.03	0.02	0.05
Total	177		1,811.80	498.84	2,310.65	0,155.32	3,981.29

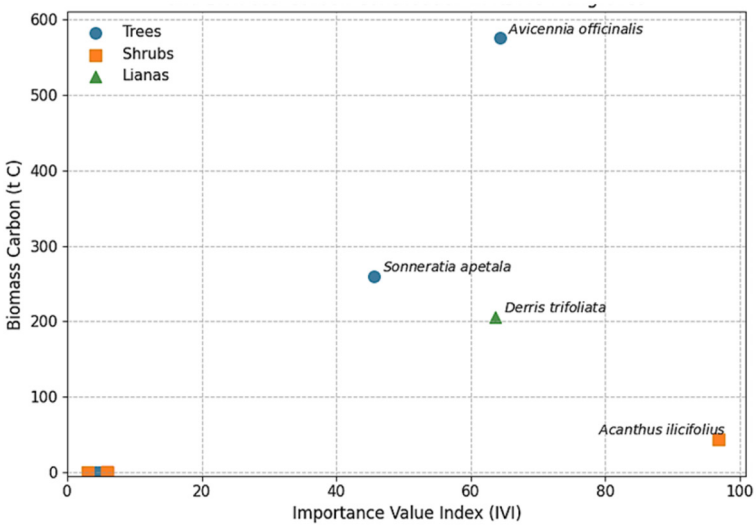

Fig. 2. Relationship between species importance (IVI) and biomass–carbon contribution.

tance (IVI) and their biomass-carbon contribution was strongly positive (Fig. 2). Dominant species with high IVI (*Avicennia officinalis, Sonneratia apetala, Derris trifoliata, Acanthus ilicifolius*) were also the largest contributors to biomass carbon storage. This pattern confirms that even in a structurally simplified, disturbed mangrove stand, phytosociological dominance is a reliable predictor of blue-carbon contribution. Minor associate species, despite being present, contributed negligibly to carbon storage due to their very low basal area and stem counts.

Soil Organic Carbon (SOC) concentration and stock distribution

Depth-wise SOC concentrations and stocks for the

Table 3. SOC (% and t C ha^{-1}) and Organic Matter (%) at two depths across stations.

Station	Coordinates (WGS 84)	%SOC (0–15 cm)	%OM (0–15 cm)	SOC (t ha^{-1}, 0–15 cm)	%SOC (15–30 cm)	%OM (15–30 cm)	SOC (t ha^{-1}, 15–30 cm)
MQ-01	19°11′58.94″ N, 73°04′13.13″ E	10.15	7.50	197.93	8.51	14.66	331.89
MQ-02	19°12′12.44″ N, 73°04′29.69″ E	11.52	19.87	224.64	13.44	23.18	524.16
MQ-03	19°12′21.37″ N, 73°04′22.34″ E	11.52	19.87	224.64	10.15	17.50	395.85
MQ-04	19°12′46.69″ N, 73°04′10.17″ E	17.29	29.80	337.16	17.83	30.75	695.37
MQ-05	19°14′08.39″ N, 73°04′25.25″ E	14.54	25.07	283.53	12.35	21.29	481.65
MQ-06	19°12′06.54″ N, 73°03′47.46″ E	17.56	30.27	342.42	15.09	26.02	588.51
MQ-07	19°12′11.39″ N, 73°04′06.02″ E	9.88	17.03	192.66	9.60	16.56	374.40
MQ-08	19°14′22.91″ N, 73°04′44.92″ E	7.13	12.30	139.04	7.41	12.77	288.99
MQ-09	19°14′05.35″ N, 73°05′38.21″ E	14.27	24.60	278.27	14.54	25.07	567.06
MQ-10	19°12′30.41″ N, 73°04′05.08″ E	12.62	21.76	246.09	13.44	23.18	524.16

Table 4. Summary statistics of SOC and related variables (n = 10 quadrats).

Variable	Mean	SD	Min	Max
%C (0–15 cm)	12.65	3.31	7.13	17.56
OM% (0–15 cm)	21.81	5.71	12.30	30.27
SOC (t ha^{-1}, 0–15 cm)	246.64	64.60	139.04	342.42
%C (15–30 cm)	12.24	3.27	7.41	17.83
OM% (15–30 cm)	21.10	5.64	12.77	30.75
SOC (t ha^{-1}, 15–30 cm)	477.20	127.46	288.99	695.37

ten stations are presented in Table 3. At 0–15 cm depth, SOC concentration ranged from 7.13% to 17.56%, while at 15–30 cm it ranged from 7.41% to 17.83%. Quadrat MQ-4 and MQ-6 had the highest SOC stocks at both depths, indicating superior carbon retention under comparatively lower disturbance and enhanced sediment retention. MQ-5 and MQ-9 showed intermediate SOC stocks, whereas MQ-7 and MQ-8 consistently had the lowest SOC at both depths, reflecting severe anthropogenic disturbance, restricted tidal exchange, and sediment compaction at those sites. Across all stations, SOC stock was higher in the 15–30 cm layer than in the 0–15 cm layer, highlighting the importance of long-term carbon burial in deeper sediment horizons.

SOC distribution and depth-wise variation

Descriptive statistics of SOC and related variables across the ten quadrats are summarized in Table 4. SOC stock in the 0–15 cm layer ranged from 139.04 to 342.42 t ha^{-1} (mean 246.64 ± 64.60 t ha^{-1}), indicating substantial surface carbon accumulation. At 15–30 cm depth, SOC stocks increased markedly, ranging from 288.99 to 695.37 t ha^{-1} (mean 477.20 ± 127.46 t ha^{-1}). The boxplot comparison (Fig. 3) clearly demonstrates the pronounced increase in SOC storage with depth. A paired t-test confirmed that SOC stocks at 15–30 cm were significantly higher than those at 0–15 cm ($t = 9.81$, $df = 9$, $p < 0.001$), highlighting the dominance of subsurface sediments in total soil carbon storage.

Relationship between surface and subsurface SOC pools

Stations with the highest surface SOC also tended to have the highest subsurface SOC. Notably, quadrats MQ-4 and MQ-6 were at the upper end of SOC for both depths, suggesting localized conditions favorable for carbon retention (e.g., finer sediments, reduced oxidation, high litter and root inputs, or sheltered hydro-geomorphic settings). Conversely, MQ-8 had the lowest SOC at both depths, implying lower organic inputs and/or more exposed sediment conditions with greater turnover. Surface and subsurface SOC stocks showed a strong positive correlation ($r = 0.904$, $p < 0.001$), indicating coherent vertical coupling of carbon accumulation across the upper 30 cm of soil. This relationship is illustrated in Fig. 4. sites with higher surface SOC also exhibit elevated subsurface SOC, suggesting that local controls on

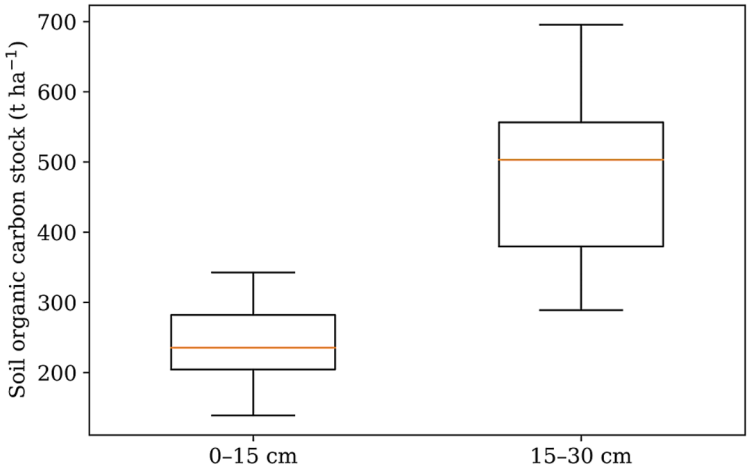

Fig. 3. Depth-wise distribution of soil organic carbon stocks (t ha^{-1}).

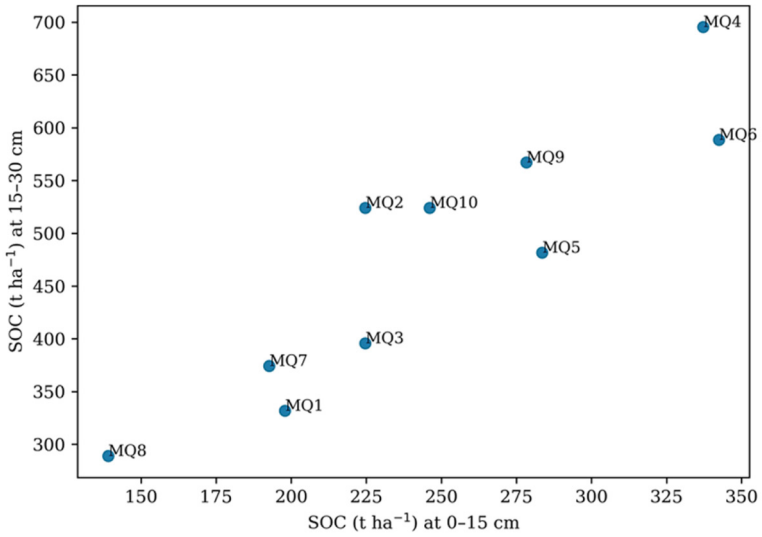

Fig. 4. Relationship between surface and subsurface SOC stocks.

organic matter input and sediment deposition operate consistently through the soil profile.

Role of carbon concentration and organic matter

SOC stocks at both depths increased proportionally with soil carbon concentration (%C) and organic matter content (%OM) (see Table 3 and Fig. 5). Given that SOC stock was calculated directly from %C (multiplying by bulk density and depth), these relationships simply reflect the quantitative dependence of SOC storage on carbon concentration, rather than independent ecological correlations. Nonetheless, the tight correspondence between %OM, %C, and SOC stock confirms that organic matter accumulation is the primary driver of carbon storage in KDMC

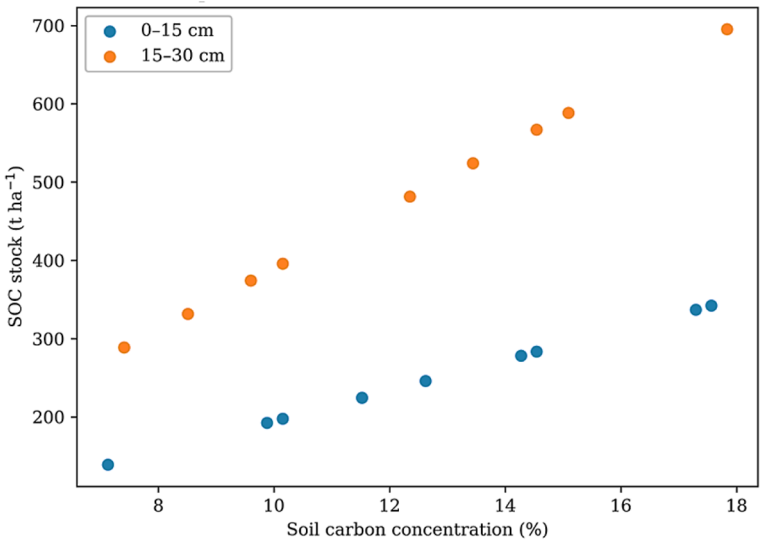

Fig. 5. %C vs SOC stocks at 0–15 cm and 15–30 cm depths.

Fig. 6. Representative anthropogenic disturbances in KDMC mangroves along the Ulhas River–Vasai–Thane Creek corridor.

mangrove soils.

Field-observed anthropogenic stressors

Field observations documented severe anthropogenic pressures in the KDMC mangroves (Fig. 6). Key stressors include solid-waste dumping, sewage discharge, embankment construction, shoreline encroachment, and intertidal land filling. These disturbances have resulted in smothering of pneumatophores, truncation of tidal channels, sediment hardening, and reduced seedling recruitment. We observed that localized canopy thinning and the dominance of shrubs and climbers were strongly associated with zones of intense disturbance.

Ecosystem service valuation

Based on a mapped mangrove extent of ~200 ± 20 ha and globally derived unit ecosystem service values, the annual ESV of the KDMC mangroves is estimated at approximately US$ 4.22 million yr^{-1} under the global mean scenario. Sensitivity analysis yields a range of roughly US$ 3.0–6.0 million yr^{-1}, reflecting uncertainties in mapped area and in the benefit-transfer valuation coefficients. When combined with the biomass carbon (~195 t C ha^{-1}) and mean SOC (~272 t C ha^{-1}) stock estimates, the total blue-carbon pool of KDMC mangroves is on the order of ~467 t C ha^{-1}. This underscores that, even in a urban-edge context, these mangroves represent a significant carbon reservoir embedded within a densely populated metropolitan landscape.

DISCUSSION

Structural reorganization of urban-edge mangrove vegetation

The phytosociological structure of the KDMC mangroves reflects a disturbance-regulated system in which shrub and liana components have progressively replaced the late-successional, tree-dominated mangrove stands. This pattern is increasingly documented in degraded urban-edge mangroves (Alongi 2015, 2022, Chen *et al.* 2021, Zhang *et al.* 2021). The

overwhelming dominance of Acanthus ilicifolius and Derris trifoliata, together with the co-dominance of Avicennia officinalis, indicates a shift from classical, tall-canopy mangrove forests toward a structurally simplified, disturbance-tolerant assemblage. Similar vegetation shifts have been reported in urban mangroves of Thane Creek and Mumbai Harbor, and in industrial estuaries of western India, where embankments, land filling, and restricted tidal flushing selectively suppress slow-growing canopy species (Nagelkerken *et al.* 2008, Shindikar *et al.* 2009, Friess *et al.* 2016a, NCSCM 2017, Lee *et al.* 2014, Alongi 2022, Kannankai *et al.* 2022, Szafranski and Granek 2023, Kumar 2025).

The very low IVI values of late-successional species like *Bruguiera cylindrica* and *Excoecaria agallocha* in KDMC suggest that hydrological truncation, propagule dispersal limitations, and substrate compaction disproportionately disadvantage these structural foundation species. Similar declines in *Bruguiera* and *Excoecaria* have been noted in the semi-arid mangroves of the Gulf of Kachchh under industrial saline stress and tidal restrictions (Thivakaran *et al.* 2020). Likewise, in fringe mangroves of the Indian Sundarbans experiencing altered flow regimes, early-stage replacement of canopy trees by disturbance-tolerant shrubs and mangrove associates has been observed (Chaudhuri *et al.* 2023). Thus, the dominance-skewed community structure (moderate Shannon diversity but high Simpson dominance) of KDMC mangroves is typical of urban-edge systems under sustained anthropogenic stress (Mukherjee *et al.* 2014, Friess *et al.* 2016a, IPCC 2019).

Ecological drivers of shrub and liana dominance

The ascendancy of the liana *Derris trifoliata* in KDMC is a clear biological signal of chronic canopy disruption and the creation of canopy gaps. Lianas are highly competitive in environments where vertical forest structure is repeatedly opened by disturbance; their rapid clonal expansion allows them to capture light and physical support effectively. Similar liana-dominated post-disturbance mangrove assemblages have been documented in Southeast Asia and urban-edge Sri Lankan estuaries, where recurrent disturbance suppresses tree regeneration and promotes climber proliferation (Satyanarayana *et al.* 2002, Schnitzer 2005, Schnitzer and Bongers 2011).

The numerical dominance of *Acanthus ilicifolius* reflects this species' extraordinary tolerance to salinity fluctuation, nutrient enrichment, periodic desiccation, and mechanical disturbance of sediments. Dense Acanthus thickets can enhance surface sediment trapping but simultaneously inhibit the recruitment of canopy-forming mangrove propagules, effectively locking the system in an arrested successional state. This feedback mechanism has been observed in disturbed mangroves of Thane Creek and in the East Kolkata Wetlands (Lee *et al.* 2014, Sumarga *et al.* 2023). Consequently, the current *Acanthus–Derris* dominated configuration in KDMC is a disturbance-adapted but carbon-fragile vegetation state, capable of short- to medium-term biomass retention, yet vulnerable to rapid collapse under intensified physical stress.

Biomass-carbon dynamics in context of other Indian mangroves

The species-wise urban-edge mangrove biomass estimates from KDMC underscore the functional primacy of the structural dominants (*Avicennia officinalis, Sonneratia apetala, Derris trifoliata,* and *Acanthus ilicifolius*) as the principal contributors to both above- and belowground biomass carbon pools. The total biomass carbon stock (~1,086 t C, or ~3,981 t CO_2e) indicates a moderate carbon sequestration capacity relative to other degraded urban mangroves in western India (Vinod *et al*. 2018, Harishma *et al.* 2020, Singh *et al.* 2023). The strong positive IVI–biomass–carbon relationship confirms that species dominance via frequency, density, and basal area disproportionately governs stand-level carbon storage, aligning with core ecological theory that links structural dominance to carbon allocation.

On a per-area basis, the KDMC biomass carbon stock (~195 t C ha^{-1}) places this system in an intermediate carbon-density class among Indian mangroves. Degraded industrial mangroves in the Gulf of Kachchh often have <150 t C ha^{-1} (Thivakaran *et al.* 2020), whereas structurally intact Sundarbans forests can exceed 300–350 t C ha^{-1} due to sustained sediment accretion and multi-tiered canopies (Chaudhuri

et al. 2023). Pichavaram mangroves similarly sustain higher biomass stocks under well-connected tidal regimes and mature stand structure (Ghosh *et al.* 2022). Within this national context, KDMC represents an intermediate, disturbance-stabilized system in which residual canopy trees (primarily *Avicennia officinalis* and *Sonneratia apetala*) continue to drive biomass accrual despite pronounced structural simplification.

The dominance of *Avicennia officinalis* (>50% of total biomass C) mirrors patterns in other urban estuaries of the MMR, where *Avicennia* thrives under high salinity and nutrient enrichment (Kauffman *et al.* 2020, Rani *et al.* 2023). Meanwhile, the substantial carbon contribution of *Derris trifoliata,* although atypical for undisturbed mangroves, reflects secondary carbon capture by lianas in the wake of repeated canopy disturbance. The stand AGB:BGB ratio of ~3.85 is within the general tropical mangrove range (Komiyama *et al.* 2008, Alongi 2020), indicating that belowground allocation remains proportionate, supporting sediment stabilization and rhizosphere functioning (Donato *et al*. 2011). These findings emphasize that even structurally simplified shrub–liana assemblages can retain substantial, if fragile, biomass carbon pools that merit protection under urban climate-mitigation frameworks.

SOC stratification in comparative framework

Our results reinforce that even in an urban-edge estuary, mangrove soils retain a large, depth-structured SOC pool. The markedly higher SOC stocks at 15–30 cm depth (mean ≈ 477 t ha^{-1}) compared to 0–15 cm (mean ≈ 247 t ha^{-1}) indicate that KDMC mangrove soils function as a significant long-term carbon sink, with carbon stabilized below the actively bioturbated surface layer. This is consistent with the known role of mangrove and estuarine sediments as effective carbon vaults due to waterlogging, anoxia, and mineral protection (Kristensen 2008, IPCC 2014, IPCC 2019, Sasmito *et al*. 2019, 2020).

The strong correlation between surface and subsurface SOC (r = 0.904) suggests that spatial controls on SOC (hydroperiod, sediment texture, organic matter input, stand structure) operate consistently through the upper soil profile. In mangroves, such coherence often reflects coupled processes: surface litter inputs and subsurface burial via sediment accretion and root turnover (Sasmito *et al.* 2019, 2020). The robust depth stratification observed confirms active carbon burial and preservation processes, which is central to blue-carbon accounting in coastal wetlands. The IPCC's wetlands supplement emphasizes quantifying soil carbon in these ecosystems because soil pools can dominate total ecosystem carbon and are vulnerable to disturbances like excavation or drainage (IPCC 2014, 2019). Deeper mangrove soil layers typically experience low oxygen, slower decomposition, greater mineral adsorption of organic matter, and continuous burial by sediment deposition and root accumulation. These mechanisms, well documented in mangrove carbon dynamics, explain the statistical depth differences we observed (Kristensen 2008, Sasmito *et al.* 2020).

A large fraction of SOC in KDMC is stored below the surface, so activities such as dredging, bund construction, land reclamation, or canalization could rapidly expose this stable carbon to oxidation, converting a carbon sink into a source. This aligns with national greenhouse gas inventory considerations for coastal wetlands (IPCC 2019). 'Hotspot' stations (e.g., MQ-4, MQ-6) that hold disproportionately high SOC should receive priority protection and monitoring. Future assessments should extend to the full 0–30 cm profile (and deeper where possible) to align with standard carbon accounting depths (FAO 2019) and to ensure long-term changes in these carbon stocks are detected.

Anthropogenic stressors and carbon-system destabilization

The field-documented stressors in KDMC mangroves: solid waste dumping, sewage effluent, tidal restriction by embankments, shoreline hardening, and infilling provide mechanistic explanations for the observed vegetation and carbon patterns. Physical barriers like embankments truncate tidal flow, suppress sediment deposition, and raise soil redox potential, thereby accelerating organic carbon oxidation and loss (Lee *et al.* 2014). Plastic and construction debris smother aerial roots (pneumatophores) and inhibit gas exchange, altering sediment microbial processes and collectively destabilizing long-term SOC storage.

Comparable urban-driven carbon loss trajectories have been observed in mangrove systems fringing major cities such as Manila Bay, Jakarta Bay, Lagos Lagoon, and the Pearl River estuary, where urban expansion has transformed persistent blue-carbon sinks into net carbon sources under episodic disturbances (Nababa *et al.* 2020, Wang *et al*. 2024). Taken together, our structural and visual indicators reinforce that degradation in the KDMC mangroves is not just a localized ecological issue but a broader socio-ecological outcome of inadequate land-use regulation, weak enforcement of coastal buffer policies, and insufficient integration of mangroves into municipal planning.

Management implications

The findings highlight that KDMC's mangroves are nearing a functional threshold beyond which carbon sink capacity, habitat quality, and resilience to sea-level rise could be irreversibly compromised. Protecting the remaining structurally dominant trees (especially *Avicennia officinalis* and *Sonneratia apetala*) and facilitating the recovery of other canopy species (*Bruguiera cylindrica, Excoecaria agallocha*) should be management priorities to re-establish vertical forest structure and long-lived biomass carbon pools. Equally critical is restoring tidal connectivity by removing or redesigning barriers and embankments, which would improve sediment delivery, maintain natural salinity regimes, and enhance propagule recruitment for forest regeneration.

Community-based monitoring and co-management initiatives can complement formal regulations by engaging local stakeholders in surveillance against encroachment and in mangrove stewardship (Mukherjee *et al.* 2014, Bunting *et al.* 2018, Damastuti *et al.* 2022, Damastuti *et al.* 2023). Targeted actions such as establishing waste-buffer zones, removing accumulated debris, and enrichment planting with native mangrove species could incrementally rehabilitate these habitats. Given the documented blue-carbon value and ecosystem services of KDMC's mangroves, they should be explicitly recognized and managed as vital urban green–blue infrastructure within municipal development and climate resilience plans.

Ecosystem-service valuation

The annual ESV of ~US$ 4.22 million for KDMC's mangroves is consistent with valuations reported for other peri-urban wetlands like the East Kolkata Wetlands, Navi Mumbai's mangroves, and Southeast Asian urban mangroves (Brander *et al.* 2012, Salem and Mercer 2012, Getzner and Islam 2020). Normalized, this equates to roughly US$ 21,000 ha^{-1} yr^{-1}, which lies within contemporary Indian mangrove value ranges (US$ 18,000–30,000 ha^{-1} yr^{-1}). Recent cost–benefit analyses have shown that urban-adjacent mangroves yield exceptionally high economic returns relative to land conversion alternatives, especially when storm protection, carbon sequestration, and fishery support services are jointly considered (Yadav *et al.* 2024). The KDMC valuation remains deliberately conservative, as it does not explicitly monetize cultural services, urban heat mitigation, or avoided property damage.

We note that manual mapping of mangrove area and reliance on global average valuation coefficients introduce uncertainty; hence the ESV estimates should be viewed as indicative magnitudes rather than precise figures. Nevertheless, they provide a robust justification for prioritizing mangrove conservation as a cost-effective nature-based investment (Brander *et al.* 2012, Salem and Mercer 2012, Getzner and Islam 2020, Alongi 2022).

Methodological uncertainties and constraints

Biomass and carbon stocks were estimated using species and growth-form appropriate allometric equations applied to inventoried individuals within fixed-area quadrats. While these models are widely accepted for mangrove ecosystems, uncertainties remain due to interspecific variability in wood density, architecture, and site-specific growth conditions, particularly for shrubs and lianas for which regionally calibrated equations are limited. Accordingly, biomass estimates for non-tree growth forms should be interpreted as conservative approximations.

The biomass carbon values reported represent aggregated stand-level estimates derived from allometric calculations and were not normalized to per-hectare units, as direct extrapolation from small sampled areas can lead to unrealistic overestimation. These values therefore reflect relative species contri-

butions and overall stand-level carbon storage rather than absolute areal density.

Soil organic carbon (SOC) stocks were quantified for the upper 30 cm of the soil profile, capturing the most biologically active layer but excluding deeper sediments that may store additional long-term carbon. Composite sampling at each station may also mask fine-scale spatial heterogeneity. Mangrove area was delineated using high-resolution satellite imagery, which carries inherent positional uncertainty despite the application of uncertainty bounds. Ecosystem service valuation relied on a benefit-transfer approach and thus does not fully account for site-specific socio-economic or non-market values.

Despite these constraints, the methodological framework provides a robust and internally consistent baseline for assessing vegetation structure, biomass carbon, and soil carbon dynamics in urban-edge mangrove systems.

Implications for urban coastal policy

KDMC's mangroves constitute critical green–blue infrastructure embedded in a rapidly urbanizing estuarine corridor. Their combined biomass–sediment carbon pool, moderate sequestration capacity, and high economic value argue for explicit inclusion in municipal climate-action plans (Akhand *et al.* 2023), disaster risk reduction strategies, and nature-based adaptation frameworks. Priority management interventions include restoring tidal connectivity, removing or modifying hydrological barriers, improving sediment quality (e.g., through pollution control and sediment supplementation if needed), establishing controlled waste-buffer zones to prevent dumping, and enrichment planting with true mangrove canopy species to enhance structural diversity. If these urban-edge mangrove systems are not stabilized, there is a risk that a long-term blue-carbon sink will be transformed into a net carbon source, especially under the pressures of ongoing urban expansion and sea-level rise.

CONCLUSION

This study provides an integrated assessment of vegetation structure, species dominance, biomass carbon, soil organic carbon (SOC), and ecosystem service value of urban-edge mangroves along the Ulhas River–Vasai–Thane Creek estuarine system within the Kalyan–Dombivli Municipal Corporation (KDMC) region. Despite persistent anthropogenic pressure, the mangrove assemblage continues to function as a measurable blue-carbon reservoir, although its structural integrity and long-term stability are increasingly constrained by urban disturbance.

Phytosociological analysis revealed a dominance of disturbance-tolerant shrubs and climbers, particularly *Acanthus ilicifolius* and *Derris trifoliata,* coupled with the reduced prevalence of late-successional canopy species (*Bruguiera cylindrica, Excoecaria agallocha*) indicating the disturbance-stabilized state. Alongside a limited number of canopy-forming mangrove trees (*Avicennia officinalis* and *Sonneratia apetala*) still account for the majority of stand biomass and carbon. The relationship between species importance and biomass carbon contribution demonstrated that ecological dominance does not uniformly translate into carbon storage potential across growth forms. Canopy-forming tree species disproportionately governed biomass carbon pools, whereas shrub- and liana-dominated components, despite high IVI values, contributed relatively little to long-term carbon storage.

Soil organic carbon constituted the dominant and more stable carbon pool, with consistently higher stocks in subsurface layers compared to surface soils. This depth-wise stratification underscores the role of mangrove sediments as long-term carbon sinks and highlights the vulnerability of these stores to physical disturbance, hydrological alteration, and land-use change. Stations exhibiting greater hydrological connectivity and reduced disturbance retained higher SOC stocks, emphasizing the importance of sedimentary integrity for blue-carbon preservation in urban mangrove systems.

The estimated ecosystem service value suggests that KDMC's mangroves provide substantial annual socio-economic benefits at the municipal scale, even under conservative valuation assumptions. Nevertheless, this valuation carries high uncertainty due to manual area delineation, variability in global unit val-

ues, and the incomplete monetization of non-market services. Thus, the ESV figures should be interpreted as policy-relevant ballpark values rather than precise economic totals.

The methodological framework adopted, combining phytosociological assessment, allometric biomass estimation, and depth-specific SOC analysis, provides a robust baseline for evaluating carbon dynamics in urban-edge mangroves. However, biomass carbon estimates represent aggregated stand-level values rather than per-hectare densities, and SOC assessments were limited to the upper 30 cm of the soil profile. These constraints necessitate cautious interpretation of absolute magnitudes, while relative patterns and species-level contributions remain ecologically meaningful and policy-relevant.

Overall, the findings indicate that KDMC mangroves represent an ecologically resilient yet carbon-fragile system, where continued degradation could rapidly erode both biomass and sedimentary carbon stocks. Conservation and restoration efforts should therefore prioritize the protection and recovery of canopy-forming mangrove species, maintenance of tidal connectivity, and prevention of physical disturbances that destabilize sediment carbon pools. The baseline generated by this study offers critical scientific support for integrating urban mangroves into municipal climate mitigation strategies, coastal resilience planning, and long-term blue-carbon conservation frameworks.

AUTHOR CONTRIBUTIONS

All authors contributed to the study conception and design. Methodology designs and laboratory analyses were undertaken by Madhuri R. Wani. Fieldwork and data collection were conducted by Madhuri R. Wani and Deepawali Shirurkar, with subsequent data analysis and interpretation performed collaboratively by all authors. The first draft of the manuscript was written by Madhuri R. Wani and all authors commented on previous versions of the manuscript. All authors read and approved of the final manuscript. Overall supervision of the research and manuscript preparation was provided by D. M. Mahajan.

ACKNOWLEDGMENTS

The authors sincerely acknowledge the Kalyan-Dombivli Municipal Corporation (KDMC) for granting permission to access and survey the area. We extend our gratitude to the Principal of Baburaoji Gholap College, Pune-27 (India), for providing essential laboratory facilities that enabled this research. We are indebted to the laboratory staff and field assistants for their valuable support in soil sampling, processing, and analysis. Special thanks are also due to colleagues and students who contributed to data collection.

REFERENCES

Akhand, A., Chanda, A., Jameel, Y., & Dasgupta, R. (2023). The present state-of-the-art of blue carbon repository in India: a meta-analysis. *Sustainability Science,* 18, 1031–1042. https://doi.org/10.1007/s11625-022-01181-4

Alongi, D. M. (2014). Carbon cycling and storage in mangrove forests. *Annual Review of Marine Science,* 6, 195–219. https://doi.org/10.1146/annurev-marine-010213-135020

Alongi, D. M. (2015). The impact of climate change on mangrove forests. *Current Climate Change Reports,* 1(1), 30–39. https://doi.org/10.1007/s40641-015-0002-x

Alongi, D. M. (2020). Carbon cycling in the world's mangrove ecosystems revisited: Significance of non-steady-state diagenesis and subsurface linkages between the forest floor and the coastal ocean. *Forests,* 11(9), 977. https://doi.org/10.3390/f11090977

Alongi, D. M. (2022). Impacts of climate change on blue carbon stocks and fluxes in Mangrove Forests. Forests, 13(2), 149. https://doi.org/10.3390/f13020149

Arathy, G. S., Prema, D., Padua, S., Kripa, V., Jeyabaskaran, R., Varghese, E., Lavanya, R., Vysakhan, P., Syamala, M. P., & John, S. (2022). Sediment blue carbon stock of Avicennia officinalis in Vembanad Lake ecosystem, Kerala, India. *Journal of the Marine Biological Association of India,* 64(2), 1–12. https://doi.org/10.6024/jmbai.2022.64.2.2220-01

Atwood, T. B., Connolly, R. M., Almahasheer, H., Carnell, P. E., Duarte, C. M., et al. (2017). Global patterns in mangrove soil carbon stocks and losses. *Nature Climate Change,* 7, 523–528. Available: http://dx.doi.org/10.1038/nclimate3326

Bandh, S. A., Malla, F. A., Qayoom, I., Mohi-Ud-Din, H., Butt, A. K., Altaf, A., Wani, S .A., Betts, R., Truong, T. H., Pham, N.D.K., Cao, D. N., & Ahmed, S. F. (2023). Importance of blue carbon in mitigating climate change and plastic/microplastic pollution and promoting circular economy. *Sustainability,* 15, 2682. https://doi.org/10.3390/su15032682.

Brander, L. M., Wagtendonk, A. J., Hussain, S. S., McVittie, A., Verburg, P. H., de Groot, R. S., & van der Ploeg, S. (2012). Ecosystem service values for mangroves in Southeast Asia: A meta-analysis and value transfer application. *Ecosystem Services,* 1(1), 62–69. https://doi.org/10.1016/j.ecoser.2012.06.003

Bunting, P., Rosenqvist, A., Lucas, R. M., Rebelo, L.-M., Hilarides,

L., Thomas, N., Hardy, A., Itoh, T., Shimada, M., & Finlayson, C. M. (2018). The Global Mangrove Watch—A New 2010 Global Baseline of Mangrove Extent. *Remote Sensing*, 10(10), 1669. https://doi.org/10.3390/rs10101669

Chaudhuri, A., Naz, A., & Maiti, S. K. (2023). Variations in soil blue carbon sequestration between natural mangrove meta populations and a mixed mangrove plantation: A case study from the world's largest contiguous mangrove forest. *Life,* 13(2), 271. https://doi.org/10.3390/life13020271

Chave, J., Coomes, D., Jansen, S., Lewis, S. L., Swenson, N. G., & Zanne, A. E. (2009). Towards a worldwide wood economics spectrum. *Ecology Letters,* 12(4), 351–366. https://doi.org/10.1111/j.1461-0248.2009.01285.x

Chave, J., Réjou-Méchain, M., Búrquez, A., Chidumayo, E., Colgan, M. S., Delitti, W. B. C., & Vieilledent, G. (2014). Improved allometric models to estimate the aboveground biomass of tropical trees. *Global Change Biology,* 20(10), 3177–3190. https://doi.org/10.1111/gcb.12629

Chen, L., Lin, Q., Krauss, K. W., Zhang, Y., Cormier, N., & Yang, Q. (2021). Forest thinning in the seaward fringe speeds up surface elevation increment and carbon accumulation in managed mangrove forests. *Journal of Applied Ecology,* 58(9), 1899–1909. https://doi.org/10.1111/1365-2664.13939

Curtis, J. T., & McIntosh, R. P. (1950). The interrelations of certain analytic and synthetic phytosociological characters. *Ecology,* 31(3), 434–455. https://doi.org/10.2307/1931497

Damastuti, E., de Groot, R., Debrot, A. O., & Silvius, M. J. (2022). Effectiveness of community-based mangrove management for biodiversity conservation: A case study from Central Java, Indonesia. *Trees, Forests and People,* 7, 100202. https://doi.org/10.1016/j.tfp.2022.100202

Damastuti, E., van Wesenbeeck, B. K., Leemans, R., de Groot, R. S., & Silvius, M. J. (2023). Effectiveness of community based mangrove management for coastal protection: A case study from Central Java, Indonesia. *Ocean & Coastal Management*, 238, 106498. https://doi.org/10.1016/j.ocecoaman.2023.106498

Donato, D. C., Kauffman, J. B., Murdiyarso, D., Kurnianto, S., Stidham, M., & Kanninen, M. (2011). Mangroves among the most carbon-rich forests in the tropics. *Nature Geoscience,* 4(5), 293–297. https://doi.org/10.1038/ngeo1123

Dutta, J., Mitra, A., Zaman, S., & Mitra, A. (2022). Stored carbon in the mangrove vegetation of Lothian Wildlife Sanctuary of Indian Sundarbans, the designated world heritage site. *Indian Forester,* 148(7), 733–741. http://doi.org/10.36808/if/2022/v148i7/151602

FAO. (2006). *Guidelines for soil description* (4th ed.). Food and Agriculture Organization of the United Nations, Rome.

FAO. (2019). Measuring and modelling soil carbon stocks and stock changes in livestock production systems: Guidelines for assessment (Version 1). Livestock Environmental Assessment and Performance (LEAP) Partnership. FAO, Rome. (CC BY-NC-SA 3.0 IGO).

Forest Survey of India (FSI). (2021). *India State of Forest Report.* Ministry of Environment, Forest and Climate Change, Government of India.

Friess, D. A., Lee, S. Y., & Primavera, J. H. (2016a). Turning the tide on mangrove loss. *Marine Pollution Bulletin,* 109(2), 673–675. https://doi.org/10.1016/j.marpolbul.2016.06.085

Friess, D. A., Thompson, B. S., Brown, B., Amir, A. A., Cameron, C., Koldewey, H. J., Sasmito, S. D., & Sidik, F. (2016b). Policy challenges and approaches for the conservation of mangrove forests in Southeast Asia. *Conservation Biology,* 30(5), 933–949. https://doi.org/10.1111/cobi.12784

Getzner, M., & Islam, M. S. (2020). Ecosystem services of mangrove forests: Results of a meta-analysis of economic values. *International Journal of Environmental Research and Public Health,* 17(16), 5830. https://doi.org/10.3390/ijerph17165830

Ghosh, S., Proisy, C., Muthusankar, G., Hassenrück, C., Helfer, V., Mathevet, R., Andrieu, J., Balachandran, N., & Narendran, R. (2022). Multiscale diagnosis of mangrove status in data-poor context using very high spatial resolution satellite images: A case study in Pichavaram mangrove forest. Tamil Nadu, India. *Remote Sensing,* 14, 2317 https://doi.org/10.3390/rs14102317 .

Harishma, K. M., Sandeep, S., & Sreekumar, V. B. (2020). Biomass and carbon stocks in mangrove ecosystems of Kerala, southwest coast of India. *Ecological Processes,* 9, 31. https://doi.org/10.1186/s13717-020-00227-8

Harris, R. J., Milbrandt, E. C., Everham, E. M., & Bovard, B. D. (2010). The effects of reduced tidal flushing on mangrove structure and function across a disturbance gradient. *Estuaries and Coasts*, 33(5), 1176–1185. https://doi.org/10.1007/s12237-010-9293-2

IPCC. (2006). *2006 IPCC Guidelines for National Greenhouse Gas Inventories.* Intergovernmental Panel on Climate Change. https://www.ipcc-nggip.iges.or.jp/public/2006gl/

IPCC. (2014). *2013 Supplement to the 2006 IPCC Guidelines for National Greenhouse Gas Inventories: Wetlands*. Intergovernmental Panel on Climate Change, Geneva, Switzerland.

IPCC. (2019). *2019 Refinement to the 2006 IPCC Guidelines for National Greenhouse Gas Inventories.* Intergovernmental Panel on Climate Change. https://www.ipcc.ch/report/2019-refinement-to-the-2006-ipcc-guidelines/

Kamruzzaman, Md., Ahmed, S., Paul, S., Rahman, Md. M., & Osawa, A. (2018). Stand structure and carbon storage in the oligohaline zone of the Sundarbans mangrove forest, Bangladesh. *Forest Science and Technology,* 14(1), 23–28. https://doi.org/10.1080/21580103.2017.1417920

Kannankai, M. P., Alex, R. K., Muralidharan, V. V., Nazeerkhan, N. P., Radhakrishnan, A., & Devipriya, S. P. (2022). Urban mangrove ecosystems are under severe threat from micro plastic pollution: a case study from Mangalavanam, Kerala, India. *Environmental Science and Pollution Research,* 29, 80568–80580. https://doi.org/10.1007/s11356-022-21530-1

Kauffman, J. B., & Donato, D. C. (2012). Protocols for the measurement, monitoring and reporting of structure, biomass and carbon stocks in mangrove forests. CIFOR Working Paper No. 86. *Center for International Forestry Research*, Bogor. https://doi.org/10.17528/cifor/003749

Kauffman, J. B., Adame, M. F., Arifanti, V. B., Schile-Beers, L. M., Bernardino, A. F., Bhomia, R. K., & Alongi, D. M. (2020). Total ecosystem carbon stocks of mangroves across broad global environmental and physical gradients. *Ecological Monographs,* 90(2), e01405. https://doi.org/10.1002/ecm.1405

Komiyama, A., Ong, J. E., & Poungparn, S. (2008). Allometry, biomass, and productivity of mangrove forests: A review.

Aquatic Botany, 89(2), 128–137. https://doi.org/10.1016/j.aquabot.2007.12.006

Kristensen, E. (2008). Mangrove crabs as ecosystem engineers, with emphasis on sediment processes. *Journal of Sea Research,* 59(1–2), 30–43. https://doi.org/10.1016/j.seares.2007.05.004

Kumar, A. (2025). Revitalizing the Wetlands of India. Progress Report 2025, India Water Foundation (p. 80).

Kusmana, C., Hidayat, T., Tiryana, T., Rusdiana, O., & Istomo. (2018). Allometric models for above- and below-ground biomass of *Sonneratia* spp. *Global Ecology and Conservation,* 15, e00417. https://doi.org/10.1016/j.gecco.2018.e00417

Lee, S. Y., Primavera, J. H., Dahdouh-Guebas, F., McKee, K., Bosire, J. O., Cannicci, S., Diele, K., Fromard, F., Koedam, N., Marchand, C., Mendelssohn, I., Mukherjee, N., & Record, S. (2014). Ecological role and services of tropical mangrove ecosystems: a reassessment. *Global Ecology and Biogeography,* 23(7), 726–743. https://doi.org/10.1111/geb.12155

Macreadie, P. I., Costa, M. D. P., Atwood, T. B., Friess, D. A., Kelleway, J. J., Kennedy, H.,... & Serrano, O. (2021). Blue carbon as a natural climate solution. *Nature Reviews Earth & Environment,* 2(11), 826–839. https://doi.org/10.1038/s43017-021-00224-1

Martin, A. J. F. (2022). Accuracy and precision in urban forestry tools for estimating total tree height. *Arboriculture & Urban Forestry,* 48(6), 319–332. https://doi.org/10.48044/jauf.2022.024

Mueller-Dombois, D., & Ellenberg, H. (1974). *Aims and Methods of Vegetation Ecology*. John Wiley & Sons. (570 pp.)

Mukherjee, N., Sutherland, W. J., Dicks, L. V., Hugé, J., Koedam, N., & Dahdouh-Guebas, F. (2014). Ecosystem service valuations of mangrove ecosystems to inform decision-making and future valuation exercises. *PLOS ONE,* 9(9), e107706. https://doi.org/10.1371/journal.pone.0107706

Nababa, I. I., Symeonakis, E., Koukoulas, S., Higginbottom, T. P., Cavan, G., & Marsden, S. (2020). Land cover dynamics and mangrove degradation in the Niger Delta region, Nigeria. *Remote Sensing,* 12(21), 3619. https://doi.org/10.3390/rs12213619

Nagelkerken, I., Blaber, S. J. M., Bouillon, S., Green, P., Haywood, M., Kirton, L. G., & Somerfield, P. J. (2008). The habitat function of mangroves for terrestrial and marine fauna: A review. *Aquatic Botany,* 89(2), 155–185. https://doi.org/10.1016/j.aquabot.2007.12.007

NCSCM (2017). Annual Report 2016–17. National Centre for Sustainable Coastal Management, Ministry of Environment, Forest & Climate Change, Chennai, India (pp 149).

Ouyang, X., Lee, S. Y., & Connolly, R. M. (2017). The role of root decomposition in global mangrove and salt-marsh carbon budgets. *Earth-Science Reviews,* 166, 53–63. https://doi.org/10.1016/j.earscirev.2017.01.004

Pachpande, S. C., & Pejaver, M. (2015). Natural carbon sequestration by dominant mangrove species Avicennia marina var. acutissima across Thane Creek, Maharashtra, India. *International Journal of Scientific & Engineering Research,* 6(2), 1162–1165*.

Panditrao (2020). Management Plan for Thane Creek Flamingo Sanctuary, Maharashtra, India. Thane Creek Flamingo Sanctuary, Maharashtra Forest Department (pp 235).

Rani, V., Nandan, S. B., Jayachandran, P. R., Preethy, C. M., Sreelekshmi, S., Joseph, P., & Asha, C. V. (2023). Carbon stock in biomass pool of fragmented mangrove habitats of Kochi, Southern India. *Environmental Science and Pollution Research,* 30(43), 96746–96762. https://doi.org/10.1007/s11356-023-29069-5

R Core Team (2023). R: A language and environment for statistical computing. R Foundation for Statistical Computing, Vienna, Austria. https://www.R-project.org/

Salem, M. E., & Mercer, D. E. (2012). The economic value of mangroves: A meta-analysis. *Sustainability,* 4(3), 359–383. https://doi.org/10.3390/su4030359

Sasmito, S. D., Taillardat, P., Clendenning, J. N., Cameron, C., Friess, D. A., Murdiyarso, D., & Hutley, L. B. (2019). Effect of land-use and land-cover change on mangrove blue carbon: A systematic review. *Global Change Biology,* 25(12), 4291–4302. https://doi.org/10.1111/gcb.14774

Sasmito, S. D., Kuzyakov, Y., Lubis, A. A., Murdiyarso, D., Hutley, L. B., Bachri, S., Friess, D. A., Martius, C., & Borchard, N. (2020). Organic carbon burial and sources in soils of coastal mudflat and mangrove ecosystems. *Catena,* 187, 104414. https://doi.org/10.1016/j.catena.2019.104414

Satyanarayana, B., Raman, A. V., Dehairs, F., Kalavati, C., & Chandramohan, P. (2002). Mangrove floristic and zonation patterns of Coringa, Kakinada Bay, East Coast of India. *Wetlands Ecology and Management,* 10(1), 25–37. https://doi.org/10.1023/A:1014345403103

Schnitzer, S. A. (2005). A mechanistic explanation for global patterns of liana abundance and distribution. *The American Naturalist,* 166(2), 262–276. https://doi.org/10.1086/431250

Schnitzer, S. A., & Bongers, F. (2011). Increasing liana abundance and biomass in tropical forests: Emerging patterns and putative mechanisms. *Ecology Letters,* 14(4), 397–406. https://doi.org/10.1111/j.1461-0248.2011.01590.x

Schnitzer, S. A., DeWalt, S. J., & Chave, J. (2006). Censusing and measuring lianas: A quantitative comparison of the common methods. *Biotropica,* 38(5), 581–591. https://doi.org/10.1111/j.1744-7429.2006.00187.x

Shindikar, M., Tetali, P., & Gunale, V. R. (2009). Habitat-based diversity assessment of mangroves of Thane Creek, West Coast, India. *The IUP Journal of Life Sciences*, 3(4), 14–27 (Available at SSRN: https://ssrn.com/abstract=1515602)

Singh, A., Kumar, R., Lakhchaura, P., Pandey, K., Ghosh, S., & Yadav, S. (2023). *Estimation of carbon stock in mangrove ecosystem.* Report by Forest Survey of India, MoEFCC, Government of India (pp 89).

Sumarga, E., Sholihah, A., Srigati, F. A. E., Nabila, S., Azzahra, P. R., & Rabbani, N. P. (2023). Quantification of ecosystem services from urban mangrove forest: A case study in Angke Kapuk, Jakarta. *Forests,* 14(9), 1796. https://doi.org/10.3390/f14091796

Szafranski, G. T., & Granek, E. F. (2023). Contamination in mangrove ecosystems: A synthesis of literature reviews across multiple contaminant categories. *Marine Pollution Bulletin,* 196, 115595. https://doi.org/10.1016/j.marpolbul.2023.115595

Taillardat, P., Friess, D. A., & Lupascu, M. (2018). Mangrove blue carbon strategies for climate change mitigation are most effective at the national scale. *Biology Letters,* 14(10),

20180251. https://doi.org/10.1098/rsbl.2018.0251

Thivakaran, G. A., Sharma, S. B., Chowdhury, A., & Murugan, A. (2020). Status, structure and environmental variations in semi-arid mangroves of India. *Journal of Forestry Research,* 31, 163-173. https://doi.org/10.1007/s11676-018-0793-4

Vinod, K., Koya, A. A., Kunhikoya, V. A., Silpa, P. G., Asokan, P. K., Zacharia, P. U., & Joshi, K. K. (2018). Biomass and carbon stocks in mangrove stands of Kadalundi estuarine wetland, south-west coast of India. *Indian Journal of Fisheries,* 65(2), 89–99. https://doi.org/10.21077/ijf.2018.65.2.72473-11

Walkley, A., & Black, I. A. (1934). An examination of the Degtjareff method for determining soil organic matter, and a proposed modification of the chromic acid titration method. *Soil Science,* 37(1), 29–38. https://doi.org/10.1097/00010694-193401000-00003

Wang, N. H., Tsai, I. C., Tseng, K. H., & Chiu, H.W. (2024). Landscape pattern changes and ecological risk assessment in five major bays of the Philippines. *Ocean & Coastal Management,* 251, 107085. https://doi.org/10.1016/j.ocecoaman.2024.107085

Yadav, P. K., Jha, P., Joy, Md. S., Bansal, T. (2024). Ecosystem health assessment of East Kolkata Wetlands, India: Implications for environmental sustainability. *Journal of Environmental Management*, 366, 121809. https://doi.org/10.1016/j.jenvman.2024.121809

Zhang, Y., Xin, K., Liao, B., Ai, X., & Sheng, N. (2021). The genetic and environmental adaptation of the associated liana species *Derris trifoliata* (Leguminosae) in mangroves. Forests, 12(10), 1375. https://doi.org/10.3390/f12101375